

## Controlling temperature in magnetic hyperthermia with low Curie temperature particles

Ioana Astefanoaei, Ioan Dumitru, Horia Chiriac, and Alexandru Stancu

Citation: [Journal of Applied Physics](#) **115**, 17B531 (2014); doi: 10.1063/1.4868709

View online: <http://dx.doi.org/10.1063/1.4868709>

View Table of Contents: <http://scitation.aip.org/content/aip/journal/jap/115/17?ver=pdfcov>

Published by the [AIP Publishing](#)

---

### Articles you may be interested in

[Effects of core/shell structure on magnetic induction heating promotion in Fe<sub>3</sub>O<sub>4</sub>/-Fe<sub>2</sub>O<sub>3</sub> magnetic nanoparticles for hyperthermia](#)

Appl. Phys. Lett. **103**, 163104 (2013); 10.1063/1.4825270

[Effect of the distribution of anisotropy constants on hysteresis losses for magnetic hyperthermia applications](#)

Appl. Phys. Lett. **103**, 142417 (2013); 10.1063/1.4824649

[Fe-based nanoparticles as tunable magnetic particle hyperthermia agents](#)

J. Appl. Phys. **114**, 103904 (2013); 10.1063/1.4821020

[Analysis of heating effects \(magnetic hyperthermia\) in FeCrSiBCuNb amorphous and nanocrystalline wires](#)

J. Appl. Phys. **111**, 07A314 (2012); 10.1063/1.3672850

[Simple models for dynamic hysteresis loop calculations of magnetic single-domain nanoparticles: Application to magnetic hyperthermia optimization](#)

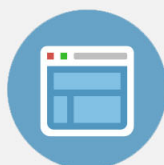
J. Appl. Phys. **109**, 083921 (2011); 10.1063/1.3551582

---



## Re-register for Table of Content Alerts

Create a profile.



Sign up today!



## Controlling temperature in magnetic hyperthermia with low Curie temperature particles

Iordana Astefanoaei,<sup>1,a)</sup> Ioan Dumitru,<sup>1</sup> Horia Chiriac,<sup>2</sup> and Alexandru Stancu<sup>1</sup>

<sup>1</sup>*Faculty of Physics, Alexandru Ioan Cuza University, Boulevard Carol I, 11, Iasi 700506, Romania*

<sup>2</sup>*National Institute of Research & Development for Technical Physics, Iasi, Romania*

(Presented 7 November 2013; received 23 September 2013; accepted 27 December 2013; published online 21 March 2014)

Hyperthermia induced by the heating of magnetic particles (MPs) in alternating magnetic field receives a considerable attention in cancer therapy. An interesting development in the studies dedicated to magnetically based hyperthermia is the possibility to control the temperature using MPs with selective magnetic absorption properties. This paper analyzes the temperature field determined by the heating of MPs having low Curie temperature (a FeCrNbB particulate system) injected within a malignant tissue, subjected to an ac magnetic field. The temperature evolution within healthy and tumor tissues was analyzed by finite element method simulations in a thermo-fluid model. The cooling effect produced by blood flowing in blood vessels was considered. This effect is intensified at the increase of blood velocity. The FeCrNbB particles, having the Curie temperature close to the therapeutic range, transfer the heat more homogeneous in the tumor keeping the temperature within the therapeutic range in whole tumor volume. Having the possibility to automatically control the temperature within a tumor, these particle type opens new research horizons in the magnetic hyperthermia. © 2014 AIP Publishing LLC. [<http://dx.doi.org/10.1063/1.4868709>]

In the last decade, various magnetic systems were studied intensively for their potential use in the magnetic hyperthermia.<sup>1–3</sup> MPs injected within malignant tissues act as smart tools for malignant cell destruction, when an alternating magnetic field is applied.<sup>4,5</sup> The idea we investigate in this paper is the thermal control using particles with low Curie temperature ( $T_c$ ). Practically, their energy absorption takes place only below  $T_c$ . A good method to stop the temperature rise beyond a required level is to use a magnetic material with low  $T_c$ . The FeCrNbB systems have been studied experimentally and their magnetic properties are detailed in Ref. 6. This paper analyzes the thermal response of a malignant tissue heated by the FeCrNbB systems when a magnetic field is applied. We have studied the temperature field determined by the heating of the particles with low Curie temperature injected within a tumor transited by a blood vessel (BV). A 3D thermo-fluid model in COMSOL Multiphysics was developed to predict the temperature within living tissues. The cooling effects due to blood flowing were considered. The heat generated through the magnetic hysteresis losses in the magnetic field was modeled using the properties determined experimentally.<sup>6</sup>

Elaboration of the 3D thermo-fluid model for a complex tumor configuration surrounded by healthy tissue is an important step in the optimization of the parameters involved in the hyperthermia treatment planning. In the present study, the temperature was computed in a geometry composed by a tumor located in a cubic region from a healthy tissue. A larger BV parallel to the z-axis was considered to transit the middle of tumor ( $x = y = 0$ ) (Fig. 1). The MPs are injected within tumor in small spherical regions assigned as injection sites. When the magnetic field is applied, the particles absorb

heat due to the hysteresis magnetic losses and transfer it to the tumor. MPs located in the injection sites convert the magnetic energy to thermal energy becoming the heating sources of the tumor.<sup>7,8</sup> The amount of heat produced in unit volume per unit time of the MPs in the alternating magnetic field with amplitude  $H$  is determined by the frequency of the field  $f$  multiplied by the hysteresis loop area in the  $M$ - $H$  coordinates (where  $M$  is MP magnetization)<sup>9,10</sup>

$$P = n f W_{loss}, \quad (1)$$

where  $n$  ( $1/m^3$ ) is density of particles loaded within tumor and hysteresis loop area is:  $W_{loss} = \mu_0 \oint H dM$ ,  $\mu_0 = 4\pi \times 10^{-7}$  H/m is the permeability. The thermal and magnetic properties of the magnetic  $Fe_{67.7}Cr_{13}Nb_{0.3}B_{20}$  particles were measured. Their specific parameters are: the mass density:  $\rho_{NMP} = 7060$  kg/m<sup>3</sup>; the specific heat capacity:  $c_{NMP} = 1227$  J/kg K; the thermal conductivity:  $k_{NMP} = 528$  W/m K, and specific saturation magnetization:  $M_s = 36$  emu/g. Using the atomic concentrations, atomic masses and densities of each alloy components, the mass density of the  $Fe_{67.7}Cr_{12}Nb_{0.3}B_{20}$  alloy was computed. The specific heat capacity and the thermal conductivity were measured using a Physical Property Measurement System (PPMS-QD9). The measuring method for the specific heat capacity is the calorimetric method. The measurement method of the thermal conductivity is the absolute one. The high values of the thermal conductivity and specific heat capacity are important in this type of application. Their thermal characteristics allow good heat propagation and a rapid thermal response of the living tissue. The spatial and temporal temperature distribution within tumour and healthy tissue is described by the solution  $T_i = T_i(x, y, z, t)$ , ( $i = 1, 2$ ) of the Pennes bioheat equation<sup>11–14</sup> with proper thermal boundary conditions at tumor-healthy tissue interface

<sup>a)</sup>Author to whom correspondence should be addressed. Electronic mail: iordana@uaic.ro.

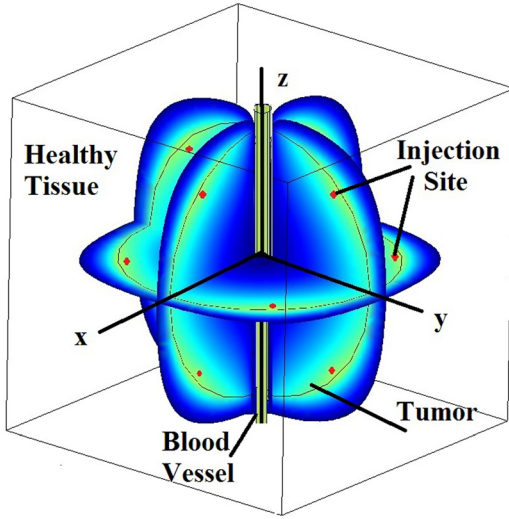


FIG. 1. Distribution of the injection sites in a tumor from healthy region.

$$\rho_i c_i \frac{\partial T_i}{\partial t} = \nabla(k_i \nabla T_i) + \rho_b w_b c_b (T_{art} - T_i) + Q_i + Q. \quad (2)$$

The index  $i=1$  denominates the tumor and index  $i=2$  denominates the healthy tissue. Equation (2) was solved by finite element method (FEM) in COMSOL Multiphysics. The following constants are:<sup>10,11</sup>

$\rho_i$ —the mass density,  $c_i$ —the specific heat capacity,  $\rho_b$ —density of blood,  $c_b$ —blood specific heat capacity,  $k_i$ —thermal conductivity,  $w_b$ —blood perfusion rate,  $T_{art}$ —arterial blood temperature,  $Q_i$ —the metabolic heat source, and  $Q$  is the volumetric heat dissipated by the MPs in the magnetic field. The heat density distribution within tumor and healthy tissue is expressed as

$$Q = \begin{cases} P, & x, y, z \in D_1 \\ 0, & x, y, z \notin D_1, \end{cases} \quad (3)$$

where  $D_1$  denotes the spatial regions of the injection sites within tumor. The heat source of the tumor is represented by the 12 injection sites (IS) where the particles are concentrated and uniformly distributed (Fig. 1). Their mass density ( $\rho_{IS}$ ), specific heat ( $c_{IS}$ ), and thermal conductivities ( $k_{IS}$ ) depend on the volume concentration  $\varnothing = n \left( \frac{4\pi R^3}{3} \right)$ , where  $n$  is the number of particles per volume and  $R$  is the particle radius<sup>14</sup>

$$\rho_{IS} = \varnothing \rho_{MNP} + (1 - \varnothing) \rho_1, \quad (4)$$

$$c_{IS} = \varnothing c_{MNP} + (1 - \varnothing) c_1, \quad (5)$$

$$\frac{1}{k_{IS}} = \frac{\varnothing}{k_{MNP}} + \frac{1 - \varnothing}{k_1}. \quad (6)$$

To investigate the thermal effect of significant BVs on temperature field of healthy and tumor tissue, the Navier-Stokes equation was solved<sup>14,15</sup>

$$\rho_b c_b \left( \frac{\partial T_b}{\partial t} + v_z \frac{\partial T_b}{\partial z} \right) = \nabla(k_b \nabla T_b) + Q, \quad (7)$$

where  $k_b$  is the blood thermal conductivity and  $v_z$  is the blood velocity.<sup>14</sup> The second term of Eq. (7) emphasizes the cooling

effect of the blood vessels within tumour which depends on the blood velocity. On the external surface of cube, the temperature,  $T_0 = 37^\circ\text{C}$  was considered (Dirichlet boundary condition). The flow velocity of blood along  $z$  direction was considered.<sup>15</sup> At tumor-vessel interfaces, the Newman boundary conditions are imposed. The heat flux coming from tumour is completely received by the BV. The continuity condition of the heat fluxes is imposed at tumour-healthy region interface and tumor-injection site interfaces, too.

Discretization of the geometry into finite elements was done. The number of elements was considered large enough (approximately  $2 \times 10^6$  elements). The discretization is realized with triangular elements, the position of the triangle nodes being an input for the FEM algorithm. The distribution of the triangular finite elements is not uniform over the considered domain, the number of elements being higher close to the boundaries. For element size, it was chosen the pre-defined meshing option from COMSOL Multiphysics, extremely fine. This option contains the following mesh size characteristics: (i) maximum element size scaling factor = 0.2; (ii) element growth rate = 1.3; (iii) mesh curvature factor = 0.2; and (iv) mesh curvature cutoff = 0.001.<sup>16</sup> A very small size of the generic finite element improves the calculus resolution at the boundaries. Using the FEM for solving the bioheat transport equation, one obtains a system of equations; the solutions are the values of the temperature in every point inside the geometric boundaries. The UMFPAK solver (available in the COMSOL Multiphysics program) was used to solve the resulting not symmetric sparse linear systems.

The temperature was computed for a spherical liver tumour located in a  $40 \text{ mm} \times 40 \text{ mm} \times 40 \text{ mm}$  cube of healthy tissue. The tumour was loaded with MPs in 12 injection sites of 0.1 mm diameter. The mass concentration was  $c = 1 \text{ mg/cm}^3$ . The injection sites are placed at the 0.5 mm from tumour periphery in an ordered distribution (Fig. 1).

The FeCrNbB particles have the Curie temperature at the value  $T_c = 43^\circ\text{C}$ . Hysteresis loop area and implicitly the power density decrease with temperature rise becoming zero at  $T_c$  temperature (Fig. 2). At this value the particles loss their ferromagnetic properties and the tissue heating is virtually stopped. This is the control mechanism of temperature within a tumor provided by the magnetic properties of the MPs.

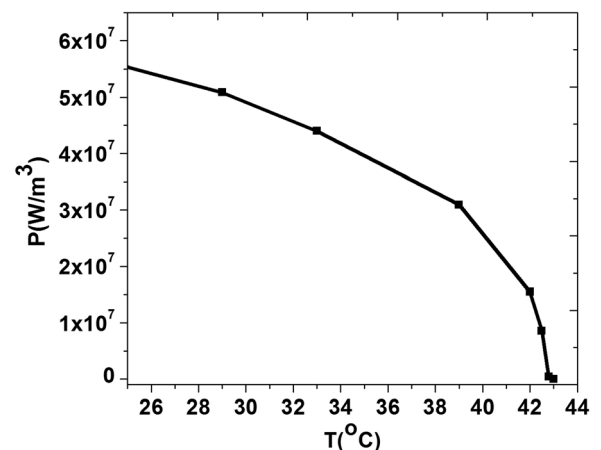


FIG. 2. The temperature dependent power density of the particles.

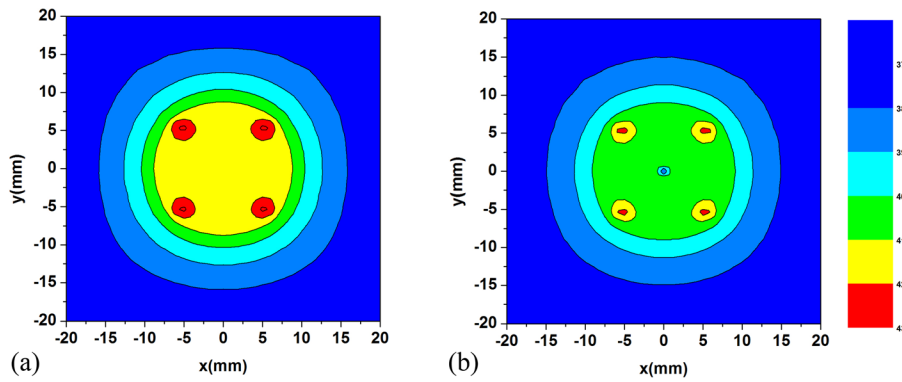


FIG. 3. The temperature within tumor for two configurations: (a) no BV and (b) one BV at the center.

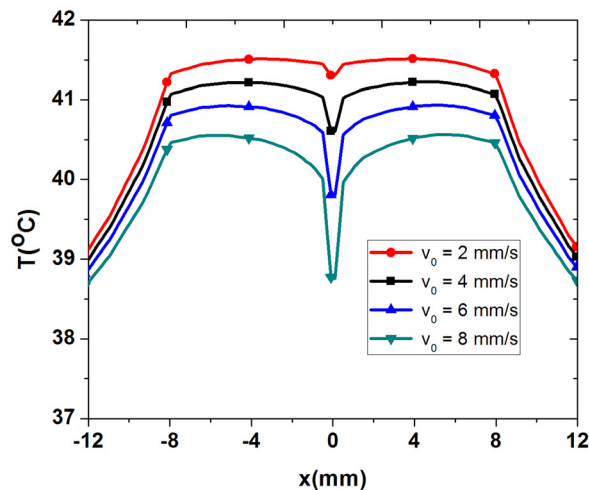


FIG. 4. The temperature ( $^{\circ}\text{C}$ ) along  $x$ -axis across the tumor for different blood velocities.

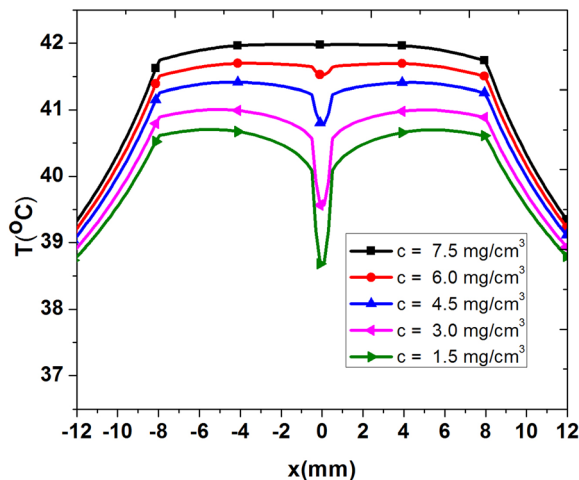


FIG. 5. The temperature ( $^{\circ}\text{C}$ ) along  $x$ -axis across the tumor for various concentrations.

The temperature field within tumor and healthy tissue was computed using the temperature dependent power density experimentally obtained in the relations (2) and (3). The temperature decreases rather abruptly at the center of tumor where the BV is located. The blood velocity in BV was considered 8 mm/s.<sup>11</sup>

Fig. 3 shows the influence of a BV with 1 mm diameter on temperature field within a tumor with diameter of 16 mm. Temperature field within the tumor without BV inside (Fig. 3(a)) is more homogeneously distributed. If a BV is located at the tumor center, the temperature decreases with a number of degrees and thermal gradients appear due to the cooling effect induced by the blood flow (Fig. 3(b)).

The cooling effect induced by BV within tumors strongly depends on the blood velocity. A higher value of blood velocity intensifies the cooling effect and thermal gradients arise within tumor (Fig. 4). The temperature values within tumor decrease for a higher blood velocity.

Fig. 5 shows the temperature along  $x$  axis across the tumor for different values of particle concentration. The temperature increases with the particle concentration. A particle concentration diminishes the cooling effect of the BV induced by the blood flowing.

The FeCrNbB systems are good candidates for hyperthermia therapy due to their magnetic and thermal properties. The temperature field within tumor can be easier controlled by these particles due to their self-regulating mechanism ( $T_c$  in the therapeutic range). The heating is virtually stopped when the particles reach the  $T_c$  temperature. The therapeutic temperature is obtained for a small value of particle concentration. All these elements are important reasons to see the FeCrNbB magnetic particles as excellent candidates in hyperthermic treatment of cancer.

This work was supported by a grant of the Romanian National Authority for Scientific Research, Parteneriate—HYPERTHERMIA Project No. 148/2012.

- <sup>1</sup>J. H. Lee *et al.*, *Nat. Nanotechnol.* **6**, 418 (2011).
- <sup>2</sup>T. Y. Liu *et al.*, *Nano Today* **4**, 52 (2009).
- <sup>3</sup>P. Cherukuri *et al.*, *Adv. Drug Delivery Rev.* **62**, 339 (2010).
- <sup>4</sup>V. A. Atsarkin and L. V. Levkin, *Int. J. Hyperthermia* **25**, 240 (2009).
- <sup>5</sup>R. Hergt *et al.*, *IEEE Trans. Magn.* **34**, 3745 (1998).
- <sup>6</sup>N. Lupu *et al.*, *IEEE Trans. Magn.* **47**, 3791 (2011).
- <sup>7</sup>Q. A. Pankhurst *et al.*, *J. Phys. D: Appl. Phys.* **36**, R167 (2003).
- <sup>8</sup>R. T. Gordon and J. R. Hines, *Med. Hypotheses* **5**, 83 (1979).
- <sup>9</sup>J. Carrey *et al.*, *J. Appl. Phys.* **109**, 083921 (2011).
- <sup>10</sup>W. Andra *et al.*, *J. Magn. Magn. Mater.* **194**, 197 (1999).
- <sup>11</sup>M. Pavel *et al.*, *IEEE Trans. Magn.* **44**, 3205–3208 (2008).
- <sup>12</sup>M. Pavel and A. Stancu, *IEEE Trans. Magn.* **45**, 4825 (2009).
- <sup>13</sup>M. Pavel and A. Stancu, *IEEE Trans. Magn.* **45**, 5251 (2009).
- <sup>14</sup>Q. Wang *et al.*, *J. Nanopart. Res.* **14**, 974 (2012).
- <sup>15</sup>M. C. Kolios *et al.*, *Phys. Med. Biol.* **40**, 477 (1995).
- <sup>16</sup>COMSOL Multiphysics, Heat Transfer Module User's Guide, pp. 145–151.